Bioorganic & Medicinal Chemistry 20 (2012) 6356–6365

Contents lists available at SciVerse ScienceDirect

Bioorganic & Medicinal Chemistry

journal homepage: www.elsevier.com/locate/bmc

Design, synthesis and biological evaluation of heterocyclic azoles derivatives containing pyrazine moiety as potential telomerase inhibitors

Yan-Bin Zhang, Xiao-Liang Wang, Wen Liu, Yu-Shun Yang, Jian-Feng Tang, Hai-Liang Zhu *

State Key Laboratory of Pharmaceutical Biotechnology, Nanjing University, Nanjing 210093, PR China

ARTICLE INFO

Article history:
Received 2 August 2012
Revised 30 August 2012
Accepted 31 August 2012
Available online 11 September 2012

Keywords:
Telomerase
Oxadiazole
Thiadiazole
Triazole
Anti-tumor activity
Pyrazine
Molecular docking

ABSTRACT

Three series of novel heterocyclic azoles derivatives containing pyrazine (**5a**–**5k**, **8a**–**8k** and **11a**–**11k**) have been designed, synthesized, structurally determined, and their biological activities were evaluated as potential telomerase inhibitors. Among the oxadiazole derivatives, compound **5c** showed the most potent biological activity against SW1116 cancer cell line (IC_{50} = 2.46 μM against SW1116 and IC_{50} = 3.55 μM for telomerase). Compound **8h** performed the best in the thiadiazole derivatives (IC_{50} = 0.78 μM against HEPG2 and IC_{50} = 1.24 μM for telomerase), which was comparable to the positive control. While compound **11f** showed the most potent biological activity (IC_{50} = 4.12 μM against SW1116 and IC_{50} = 15.03 μM for telomerase) among the triazole derivatives. Docking simulation by positioning compounds **5c**, **8h** and **11f** into the telomerase structure active site was performed to explore the possible binding model. The results of apoptosis demonstrated that compound **8h** possessed good antitumor activity against HEPG2 cancer cell line. Therefore, compound **8h** with potent inhibitory activity in tumor growth inhibition may be a potential antitumor agent against HEPG2 cancer cell. Therefore, the introduction of oxadiazole, thiadiazole and triazole structures reinforced the combination of our compounds and the receptor, resulting in progress of bioactivity.

1. Introduction

Telomerase is a ribonucleoprotein for telomere maintenance which utilizes its RNA component as the template to extend telomeric DNA length.[1] The activity of telomerase could be detected in about 85–90% of tumor cells, whereas it is low or not present in most somatic cells.[2] This is not surprising since one of the hallmarks of tumor is the indefinite growth managed by preventing telomere shortening and senescence.[3] Thus, the maintenance of telomere length is considered as a biological marker for determining the proliferation of cancer cells.[4] The essential role of telomerase in cancer and ageing makes it an important target for the development of therapies to treat cancer and other age-associated disorders.[5]

Pyrazine is the heterocyclic compound having two nitrogen atoms in the *para*-position of the six-membered ring. Ligands containing a pyrazine ring are widely studied and their π-donor properties are interesting.[6] Pyrazine has been paid great attention, because the diazine rings form an important class of compounds presented in several natural and synthetic compounds.[7] Pyrazine derivatives have been widely used in the fields of medicinal chemistry for the skeleton of biologically active sites.[8,9] Pyrazine was used to replace benzo[*b*]dioxin mainly according to the result of CADD (computer assistant drug design) method. The result indicated that a smaller moiety with higher electronic density might improve the bioactivity.

1,3,4-Oxadiazoles are an important class of heterocyclic compounds with a wide range of biological such as antiviral,[10] antimicrobial,[11] fungicidal,[12] anticancer,[13,14] tyrosinase inhibitory[15] activities. Further, 1,3,4-oxadiazole heterocycles are very good bioisosteres of amides and esters, which can contribute substantially in increasing pharmacological activity by participating in hydrogen bonding interactions with the receptors.[16] 1,3,4-Thiadiazole nucleus constitutes the active part of several biologically active compounds, including anticancer,[17,18] antibacterial[19] and anti-inflammatory agents.[20] Moreover, the introduction of different heterocyclic backbone to the thiadiazole nucleus will affect its biological activity, which has drawn widespread attention.[21] The chemistry of N-bridged heterocycles derived from 1,2,4-triazole has received considerable attention in recent years due to their usefulness in different areas of biological activities and as industrial intermediates.[22] The derivatives of 1,2,4-triazole possess a wide range of antimicrobial[23,24] and antitumour[25,26] activities. Recently, the compounds containing 1,2,4-triazole were discovered as a novel class of potent tubulin polymerization inhibitors.[27,28] 1,3,4-Thiadiazole and 1,2,4-triazole were introduced to see if 1,3,4-oxadiazole could be replaced by a similar heterocyclic one, thus, to seek for more potent telomerase inhibitors.

Some 1,3,4-oxadiazole derivatives have been reported as potential telomerase inhibitors.[29,30] However, to our knowledge, few reports have been dedicated to the synthesis and telomerase

* Corresponding author. Tel.: +86 25 8359 2572; fax: +86 25 8359 2672.
E-mail address: zhuhl@nju.edu.cn (H.-L. Zhu).

0968-0896/$ - see front matter © 2012 Elsevier Ltd. All rights reserved.
http://dx.doi.org/10.1016/j.bmc.2012.08.059

structure inhibitory activity of heterocyclic azoles derivatives containing pyrazine. Herein, in continuation to extend our research on antitumor compounds with telomerase structure inhibitory activity, in the present work we sought to synthesis three series of heterocyclic azoles derivatives containing pyrazine as antitumor agents, besides, we discussed the differences of biological activities among the three series, oxadiazoles, thiadiazoles, and triazoles. Biological evaluation indicated that some of the synthesized compounds were potent inhibitors of telomerase structure.

2. Results and discussion

2.1. Chemistry

In this study, thirty-three heterocyclic azoles derivatives containing pyrazine were synthesized. The synthetic routes of compounds **5a**–**5k**, **8a**–**8k** and **11a**–**11k** were shown in Scheme 1.

It was prepared in several steps. Firstly, esterification of the 2-pyrazine carboxylic acid **1** with methanol and concentrated sulfuric acid afforded the corresponding ester **2**. The pyrazine-2-carbohydrazide **3** was obtained by reacting **2** with 85% hydrazine monohydrate in ethanol. Then oxadiazole, thiadiazole and triazole derivatives containing pyrazine were systhesized from the pyrazine-2-carbohydrazide **3**. Treatment of the hydrazide **3** with carbon disulfide in the presence of KOH and 95% ethanol under reflux gave the intermediate **4**. The synthesis of compounds **5a**–**5k** was accomplished by refluxing **4** with halogen-substituted benzyl bromide in the presence of K_2CO_3 in acetone. The hydrazide **3** was stirred with KOH in absolute methanol, and carbon disulfide was slowly added, then compound **6** was precipitated. Dried compound **6** was stirred in concentrated sulfuric acid at 0 °C, the mixture was then poured into ice-water, obtaining the intermediate **7**. The synthesis of compounds **8a**–**8k** was accomplished by refluxing **7** with halogen-substituted benzyl bromide in the presence of K_2CO_3 in acetone. A mixture of the hydrazide **3** and phenyl isothiocyanate was refluxed in ethanol for 30 min. The solution was cooled and compound **9** was precipitated. A solution of NaOH (2 N) containing **9** was stirred under refluxing for 30 min, yielding the desired compound **10**. Then, eleven 1,2,4-triazole derivatives (**11a**–**11k**) were prepared by refluxing in anhydrous acetonitrile of **10** with halogen-substituted benzyl bromide compounds.

All of the synthetic compounds gave satisfactory analytical and spectroscopic data, which were in full accordance with their depicted structures. Additionally, the structure of compounds **5k**, **8k**, **11e** and **11i** were further confirmed by X-ray diffraction. The crystal data are presented in Table 1 and Figure 1, which give a perspective view of these compounds together with the atomic labeling system.

2.2. Biological activity

2.2.1. Anti-proliferation assay

All the synthesized heterocyclic azoles derivatives were evaluated for their anti-proliferative activity against the HEPG2 (human liver cancer cell), SW1116 (human colorectal carcinoma cell), HELA (human cervical cancer cell) and BGC823 (human gastric cancer). The results were summarized in Table 2.

As illustrated in Table 2, the active analogs showed a distinctive potential pattern of selectivity as well as broad-spectrum antitumor activity. With regard to selectivity against individual cell lines, most of the compounds showed better activities against cell lines HEPG2 and SW1116 than HELA and BGC823 with lower IC_{50} values. Especially, these compounds showed effectiveness against cell line human hepatocellular liver carcinoma HEPG2 with IC_{50} values range of 0.78–22.57 μM comparative to staurosporine (1.30 μM). Among these compounds, compound **8h** showed the most potent biological activity (IC_{50} = 0.78 μM). Overall, series **8a**–**8k** mostly showed better activities against the cell lines than series **5a**–**5k** and **11a**–**11k**, but not absolutely. When regarding HEPG2 cell line, IC_{50} values of compounds **8e**, **8g**, **8h** and **8j** ranged of 0.78–6.90 μM, compared with **5c**, **5d**, **5e** (4.22–7.50 μM) and **11e**, **11f**, **11i** (10.07–10.64 μM). Also, the same regular pattern was observed with compounds **8e**, **8g**, **8h** and **8i** with IC_{50} values range of 1.47–5.26 μM, comparable with **5c**, **5d**, **5e** (2.46–7.88 μM) and **11d**, **11f**,

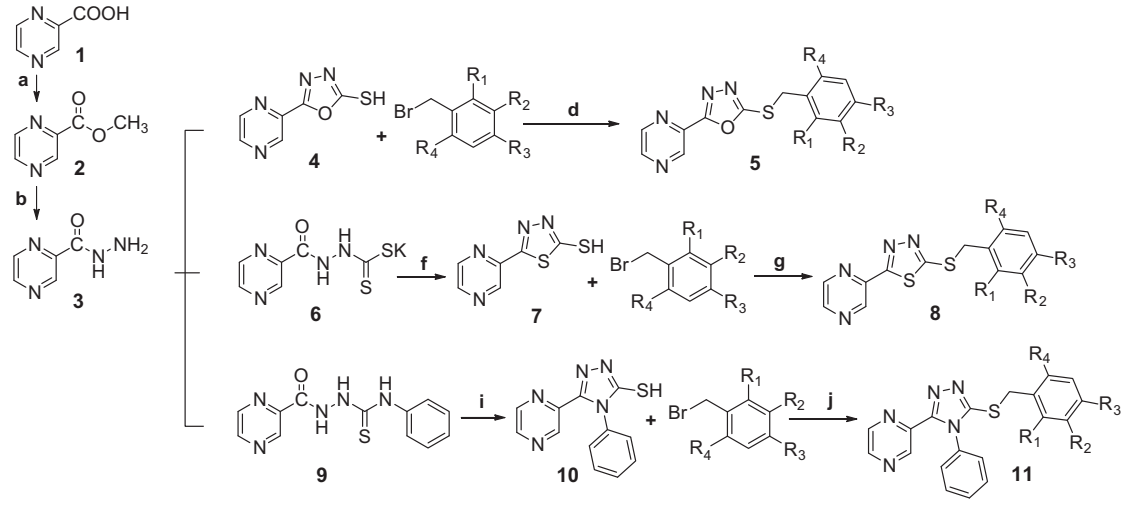

5a/8a/11a	R_1=F, R_2=R_3=R_4=H	**5b/8b/11b**	R_1=Cl, R_2=R_3=R_4=H	**5c/8c/11c**	R_1=Br, R_2=R_3=R_4=H
5d/8d/11d	R_2=Cl, R_1=R_3=R_4=H	**5e/8e/11e**	R_2=Br, R_1=R_3=R_4=H	**5f/8f/11f**	R_3=F, R_1=R_2=R_4=H
5g/8g/11g	R_3=Cl, R_1=R_2=R_4=H	**5h/8h/11h**	R_3=Br, R_1=R_2=R_4=H	**5i/8i/11i**	R_1=R_3=F, R_2=R_4=H
5j/8j/11j	R_1=R_4=F, R_2=R_3=H	**5k/8k/11k**	R_1=R_2=R_3=R_4=H		

Scheme 1. General synthesis of compounds (**5a**–**5k**, **8a**–**8k** and **11a**–**11k**). Reagents and conditions: (a) methanol, concentrated sulfuric acid; reflux, 8–12 h; (b) $NH_2NH_2{\cdot}H_2O$ (85%), ethanol; reflux, 8–12 h; (c) (1) CS_2/KOH, ethanol (95%), reflux, 24 h, (2) HCl, pH 5–6; (d) K_2CO_3, acetone, reflux, 1 h; (e) methanol, KOH, CS_2, rt; (f) concentrated sulfuric acid, 0 °C; (g) K_2CO_3, acetone, reflux, 1 h; (h) phenyl isothiocyanate, ethanol, reflux, 30 min; (i) NaOH (2 N), reflux, 30 min; (j) reflux, acetonitrile.

Table 1
Crystallographical and experimental data for compounds **5k**, **8k**, **11e** and **11i**

Crystal parameters	Compound **5k**	Compound **8k**	Compound **11e**	Compound **11i**
Formula	$C_{13}H_{10}N_4OS$	$C_{13}H_{10}N_4S_2$	$C_{19}H_{14}BrN_5S$	$C_{19}H_{14}F_2N_5S$
Formula weight	270.32	286.39	424.32	381.41
Crystal system	Monoclinic	Monoclinic	Monoclinic	Monoclinic
Space group	$P2_1/n$	$P2_1/n$	$P2_1/c$	$P2_1/c$
α (°)	90	90	90	90
β (°)	110.054(7)	101.575(5)	107.906(18)	90.468(10)
γ (°)	90	90	90	90
a (Å)	7.607(5)	5.808(4)	14.27(3)	16.022(18)
b (Å)	17.209(11)	29.459(18)	13.49(3)	10.288(12)
c (Å)	10.265(7)	7.882(5)	9.847(19)	10.868(12)
V (Å)	1262.3(14)	1321.2(15)	1804(7)	1789(4)
Z	4	4	4	4
Calculated density (Mg/cm^3)	1.422	1.440	1.562	1.416
Mu(MoKa) (mm^{-1})	0.253	0.393	2.407	0.215
Absorption coefficient (mm^{-1})	0.756	0.767	9.983	0.760
F (000)	560.0	592	856	784
θ range (°)	2.37–28.14	2.73–28.33	2.65–26.50	2.35–29.05
hkl limits	$-9 \leqslant h \leqslant 10$, $-22 \leqslant k \leqslant 18$, $-13 \leqslant l \leqslant 8$	$-7 \leqslant h \leqslant 7$, $-39 \leqslant k \leqslant 38$, $-9 \leqslant l \leqslant 10$	$-17 \leqslant h \leqslant 16$, $-15 \leqslant k \leqslant 16$, $-12 \leqslant l \leqslant 12$	$-20 \leqslant h \leqslant 21$, $-13 \leqslant k \leqslant 13$, $-14 \leqslant i \leqslant 11$
Reflections collected/ unique	6361/2861 [R_{int} = 0.052]	11246/3216 [R_{int} = 0.039]	9979/3669 [R_{int} = 0.083]	13649/4427 [R_{int} = 0.060]
Data/restraints/ parameters	2861/0/172	3216/0/172	3669/0/235	4427/0/244
R_1/wR_2 [$I > 2\sigma(I)$]	0.0640/0.1339	0.0525/0.1156	0.1695/0.1863	0.1867/0.4226
R_1/wR_2 (all data)	0.1255/0.1682	0.0721/0.1241	0.0629/0.1419	0.1323/0.3748
GOF	1.069	1.065	0.994	1.488

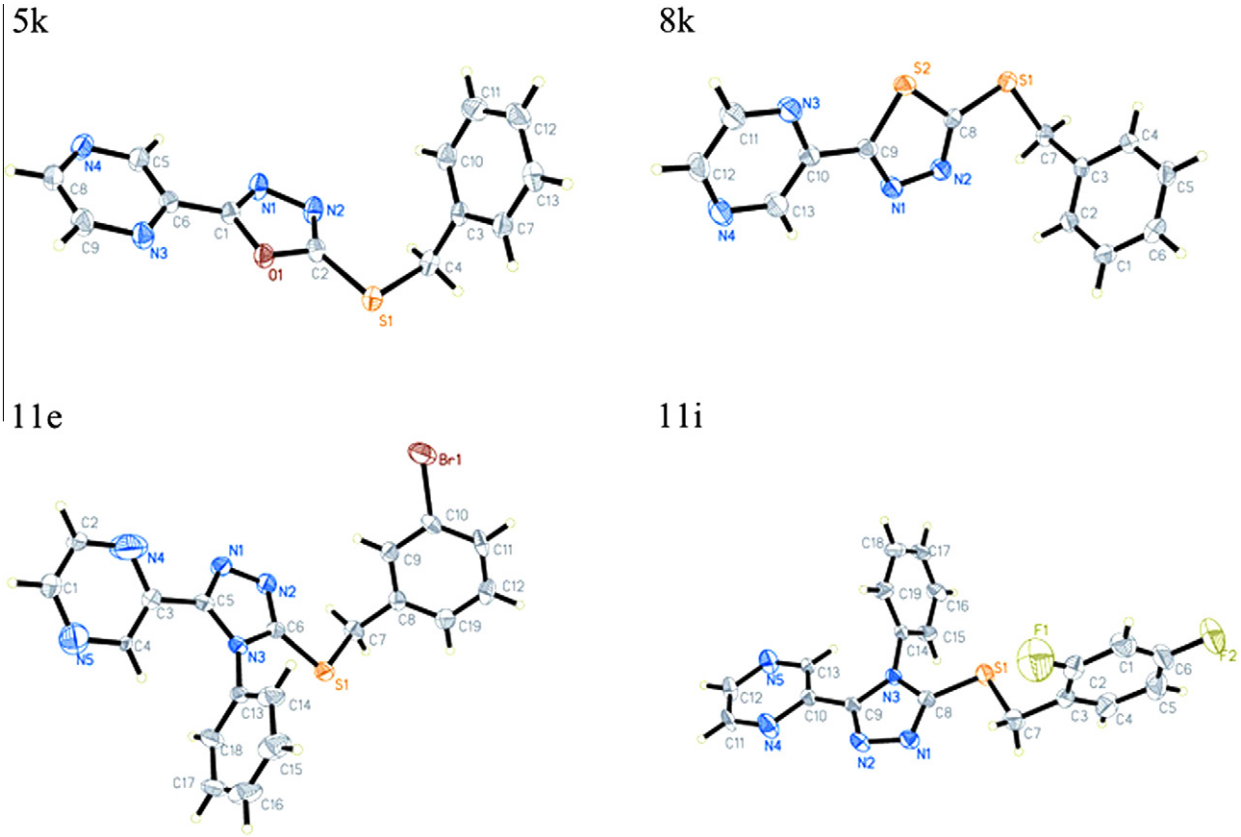

Figure 1. Crystal structure diagrams of compounds **5k**, **8k**, **11e** and **11i**.

11i (4.12–6.61 μM) against SW1116 cell line. HELA cell line was proved to be sensitive toward **11e**, **11f** and **11h** with IC_{50} concentration range of 7.30–9.58 μM comparative with **5c**, **5d**, **5k** (8.89–21.12 μM) and **8e**, **8g**, **8h** (5.43–18.87 μM). BGC823 cell line was seemed to be less effective to compounds **8d**, **8g** and **8i** with IC_{50} concentration range of 13.45–14.65 μM together with

Table 2
Antiproliferative activity of the synthesized compounds (**5a**–**5k**, **8a**–**8k** and **11a**–**11k**)

Compounds	$IC_{50}(\mu M)$			
	HEPG2	SW1116	HELA	BGC823
5a	12.47	16.78	25.33	18.18
5b	12.29	15.08	23.01	27.73
5c	4.22	2.46	8.89	17.55
5d	7.50	7.88	14.63	15.75
5e	5.79	5.06	30.31	11.48
5f	16.46	22.66	41.64	>50
5g	11.47	17.29	24.61	30.01
5h	13.21	14.43	21.57	25.68
5i	14.41	19.28	26.72	33.04
5j	17.13	23.76	>50	>50
5k	11.21	34.00	21.12	25.04
8a	9.52	6.77	32.67	18.43
8b	10.78	7.53	28.86	20.33
8c	9.81	6.95	21.30	18.86
8d	7.03	12.09	29.73	14.65
8e	1.79	5.26	5.43	16.72
8f	10.12	17.13	>50	29.33
8g	6.23	4.77	18.87	13.43
8h	0.78	1.47	12.36	25.18
8i	9.63	5.18	20.90	14.45
8j	6.90	16.83	29.17	18.59
8k	11.35	7.88	34.40	21.20
11a	19.27	18.84	44.10	>50
11b	18.83	18.13	>50	34.66
11c	11.63	19.39	>50	36.24
11d	19.62	6.61	13.52	20.26
11e	10.64	5.03	9.58	18.29
11f	10.07	4.12	7.30	27.15
11g	15.34	12.54	>50	27.67
11h	11.38	6.21	8.63	19.76
11i	10.41	4.65	12.53	17.82
11j	22.57	24.11	>50	>50
11k	17.14	15.42	35.55	>50
5-Fluorouracil	1.30	2.41	3.25	1.52
Staurosporine	6.73	4.95	9.12	6.83

compounds **5c**, **5d**, **5e** (11.48–17.55 μM) and compounds **11e**, **11h**, and **11i** (17.82–19.76 μM). It was concluded that compounds **5c**, **5d**, **8e**, **8g**, **8h**, **11e**, **11f**, **11h** and **11i** showed broad-spectrum antitumor activity with IC_{50} concentration range of 0.78–27.15 μM against the mentioned four cancer cell lines.

Subsequently preliminary SAR (structure–activity relationship) studies were performed to deduce how the structure variation (oxadiazole, thiadiazole, and triazole) and different halogen atom substituent could affect the anticancer activity. Through investigating on the selectivity of the tested compounds over the four cell lines, it was clear that the tested compounds showed stronger activities against HEPG2 than other three cancer cell lines. Among the tested compounds, compound **8h** showed the most potent biological activity against HEPG2 cancer cell line with IC_{50} value of 0.78 μM. Some rules were summarized, respectively, in different skeletons (oxadiazole, thiadiazole, and triazole) with different halogen atom substituent on benzene ring against the four cell lines, the rules were quite different, but not absolutely, which might lead to different antitumor activity. With regard to the 1,3,4-oxadiazole derivatives **5a**–**5k**, comparisons of antitumor activities with different halogen atoms substituent on benzene ring were demonstrated as follows: when the compounds were *ortho*-position halogen-substituted derivatives, the potency order was Br > Cl = F (e.g., **5a**, **5b**, **5c**) and among the *meta*-position halogen-substituted compounds the potent inhibitory action order could be summarized as Br > Cl (e.g., **5d**, **5e**); while when the substitute happened on the *para*-position of benzene ring, the potency order was Cl > Br > F (e.g., **5f**, **5g**, **5h**). The rules were quite similar to the 1,3,4-thiadiazole derivatives **8a**–**8k**, possibly because their structures were very alike. The difference was just on the *ortho*-position, which presented as F = Br > Cl (e.g., **8a**, **8b**, **8c**). However, the potent inhibitory activity order of 1,2,4-triazole derivatives **11a**–**11k** with halogen atom substituent was quite different from the compounds mentioned before. Among the *meta*-position halogen-substituted compounds, the potent inhibitory action order could be summarized as Br > Cl (e.g., **11d**, **11e**); while when the substitute happened on the *para*-position, the potency order was F > Br > Cl (e.g., **11f**, **11g**, **11h**), but the potency was not very obvious when happened on *ortho*-position. Overall, most Br-substituted compounds showed better activities than other halogen-substituted compounds, like compounds **5c**, **5h**, **8c**, **8e**, **8h**, **11e** and **11h** with IC_{50} values ranged of 0.78–25.68 μM. The same halogen atom substituent on different positions of benzene ring also presented quite different orders in different skeletons. With regard to the Br-substituted compounds, no similarities were found as follows: *ortho* > *meta* > *para* (e.g., **5c**, **5e**, **5h**) in 1,3,4-oxadiazole derivatives, *para* > *meta* > *ortho* (e.g., **8c**, **8e**, **8h**) in 1,3,4-thiadiazole derivatives and *meta* > *para* = *ortho* (e.g., **11c**, **11e**, **11h**) in 1,2,4-triazole derivatives. While the potent inhibitory activity orders of compounds with Cl-substituted on the benzene ring were *meta* > *para* = *ortho* (e.g., **5b**, **5d**, **5g**) in 1,3,4-oxadiazole derivatives, *para* > *meta* > *ortho* (e.g., **8b**, **8d**, **8g**) which was similar to the Br-substituted compounds in 1,3,4-thiadiazole derivatives, and *para* > *ortho* = *meta* (e.g., **11b**, **11d**, **11g**) in triazole derivatives. However, the potent inhibitory activity orders were uncertain of F-substituted compounds, the potency order of fluorine substituted 1,2,4-triazole derivatives was summarized as *ortho* > 2,4-disubstituded > *para* = 2,6-disubstituded. The results showed that Br-substituted on benzene ring could enhance the activity of compounds, but the position of bromine atom was not absolutely. It could be a promising lead for the further development of novel telomerase inhibition agents.

2.2.2. Telomerase inhibition assay

In addition, we also selected 15 compounds which had better or worse anti-proliferative activity to test their telomerase inhibitory activity against HEPG2 cell line. The results were summarized in Table 3. Most of the tested compounds displayed potent telomerase inhibitory. Among them, compound **8h** showed the most potent inhibitory activity with IC_{50} of 1.24 μM. Then, an analysis between telomerase inhibition and inhibition of HEPG2 cellular proliferation of the selected 15 compounds indicated that there was a moderate correlation between telomerase inhibition and inhibition of HEPG2 cellular proliferation with *R* square value of 0.839. The results of telomerase inhibitory activity of the tested compounds were corresponding to the structure relationships of their antitumor activities. This demonstrated that the potent

Table 3
Telomerase inhibitory activity of selected compounds

Compounds	Telomerase inhibitation (IC_{50}, μM)
5c	3.55
5d	6.38
5e	3.59
5f	17.12
8c	3.97
8d	3.12
8e	1.54
8f	12.09
8g	7.88
8h	1.24
11a	17.65
11f	15.03
11g	13.44
11h	7.13
11j	24.16
Staurosporine	4.14

antitumor activities of the synthetic compounds were probably correlated to their telomerase inhibitory activities.

2.2.3. Apoptosis assay

Apoptosis is an essential mechanism used to eliminate activated HEPG2 cells during the shutdown process of excess immune responses and maintain proper immune homeostasis, while deficient apoptosis of activated HEPG2 cells is associated with a wide variety of immune disorders. We detected the mechanism of compound **8h** (Fig. 2) inhibition effects by flow cytometry (FCM), and found that the compound could induce the apoptosis of activated HEPG2 cells in a dose dependent manner. The result indicated that compound **8h** induced apoptosis of antitumor stimulated HEPG2 cells.

2.3. Binding models of compounds 5c, 8h and 11f into telomerase

To gain better understanding on the potency of the synthesized compounds and guide further structure–activity relationships (SARs) studies. The molecular docking was performed by potent inhibitor **5c** (Fig. 3A), **8h** (Fig. 3B) and **11f** (Fig. 3C) into binding site of telomerase. All docking runs were applied Discovery Studio 3.1 (DS 3.1). In the binding model, compound **5c** is nicely bound to the telomerase with five hydrogen bonds. The amino hydrogen atom of Arg 194 forms two hydrogen bonds with the two nitrogen atoms of oxadiazole group at the same time. Also, the oxygen atom of the oxadiazole group and the amino hydrogen atom of Gln 308 form another hydrogen bond interaction, which means the oxadiazole group plays an impotant part in the combination of the receptor and ligand. Besides, the two amino hydrogen atoms of Lys 189, respectively, from two hydrogen bonds with the nitrogen atom of pyrazine group. Compound **8h** is also nicely bound to the telomerase with four interactions. The amino hydrogen atom of Arg 194 forms two hydrogen bonds with the two nitrogen atoms of thiadiazole group at the same time. Also the amino hydrogen atom of Gly 309 forms a hydrogen bond with the nitrogen atom of pyrazine group. Besides, the benzene ring of compound **8h** forms a π-cation interaction with Lys 189. This ensures the binding affinity and results in an increased telomerase inhibitory activity. In addition, Compound **11f** is nicely bound to the telomerase with five interactions. The amino hydrogen atom of Arg 194 also forms two hydrogen bonds with the two nitrogen atoms of thiadiazole group at the same time. Besides, another amino hydrogen atom of Arg 194 forms a π-cation interaction with the pyrazine ring. The sulfur atom between the benzene ring and triazole ring forms a hydrogen bond with the nitrogen atom of Gln 308. The amino hydrogen atom of Lys 189 forms a hydrogen bond with the fluorine atom of the benene ring. In summary, the choosed heterocyclic azoles derivatives containing pyrazine are nicely combined to the telomerase, Arg 194 and Lys 189 play an important part in the combination of the receptor and ligand. These results, along with the data of inhibitory activity assay indicated that compounds **5c**, **8h** and **11f** would be a kind of potential inhibitor.

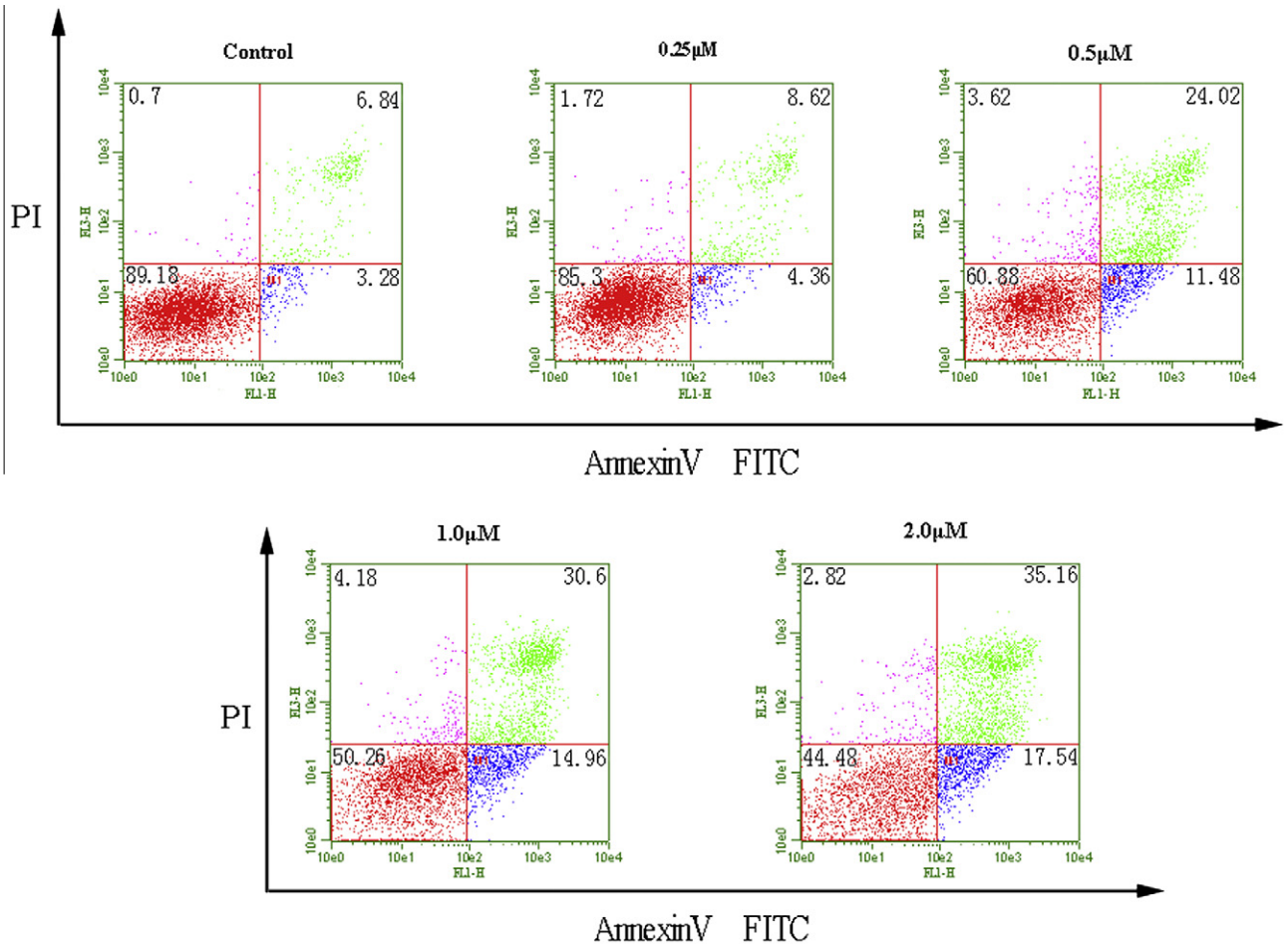

Figure 2. HEPG2 cells isolated from naïve mice were cultured with anticancer and various concentrations of **8h** for 24 h. Cells were stained by Annexin VeFITC/PI and apoptosis was analyzed by flow cytometry.

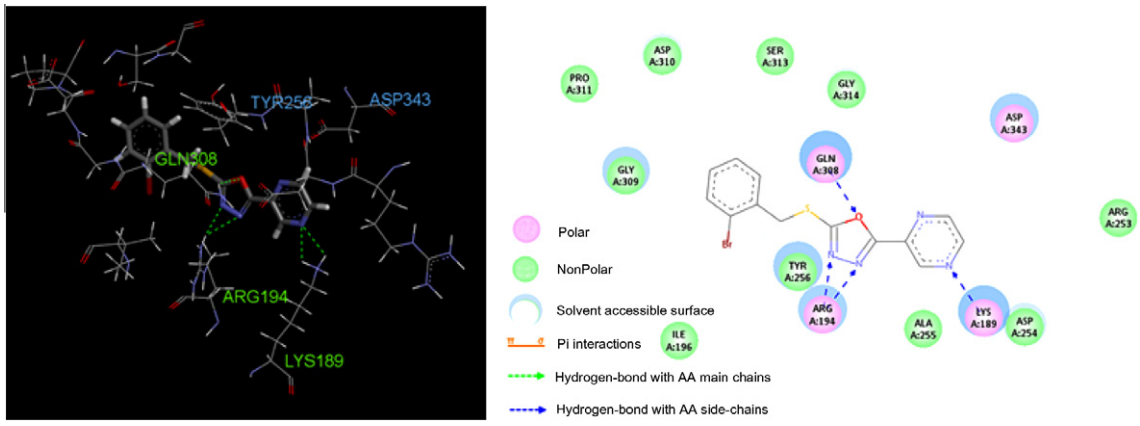

Figure 3A. Left: 3D model of the interaction between compound **5c** and the 3DU6 binding site. The H-bond (green lines) is displayed as dotted lines. Right: 2D molecular docking modeling of compound **5c** with 3DU6. The H-bond (blue arrows) is displayed as dotted arrows.

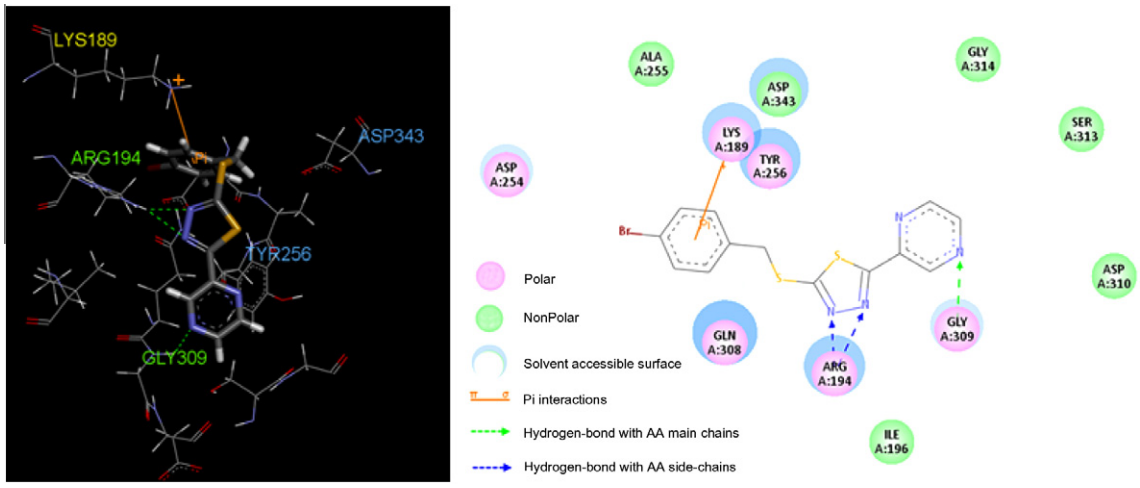

Figure 3B. Left: 3D model of the interaction between compound **8h** and the 3DU6 binding site. The H-bond (green lines) is displayed as dotted lines, and the π-cation interactions are shown as orange lines. Right: 2D molecular docking modeling of compound **8h** with 3DU6. The H-bond (blue or green arrows) is displayed as dotted arrows, and the π-cation interactions are shown as orange lines.

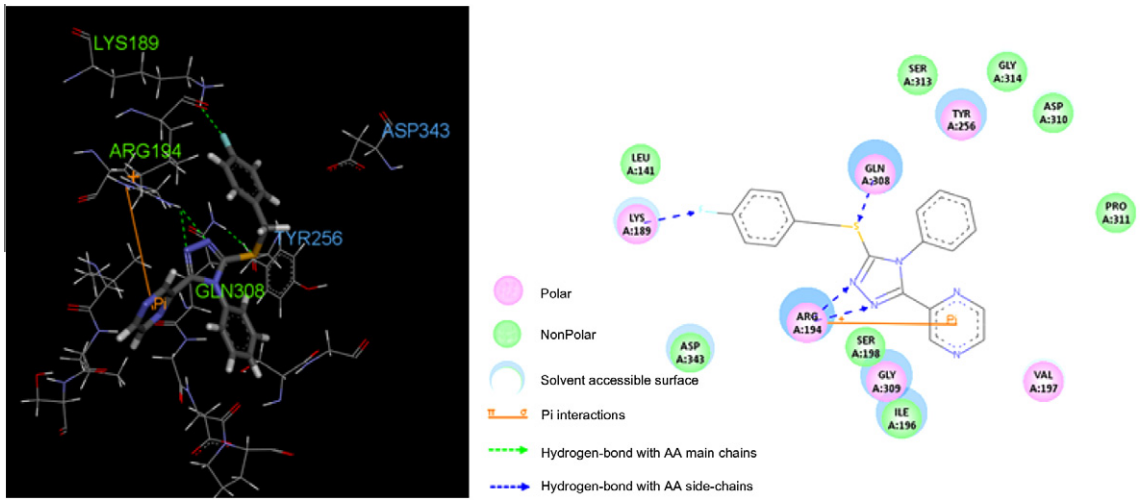

Figure 3C. Left: 3D model of the interaction between compound **11f** and the 3DU6 binding site. The H-bond (green lines) is displayed as dotted lines, and the π-cation interactions are shown as orange lines. Right: 2D molecular docking modeling of compound **11f** with 3DU6. The H-bond (blue arrows) is displayed as dotted arrows, and the π-cation interactions are shown as orange lines.

3. Conclusions

Three series of heterocyclic azoles derivatives containing pyrazine have been synthesized and evaluated for their antitumor activities. Compound **5c** demonstrated potent inhibitory activity that inhibited the growth of HEPG2 cells with IC_{50} of 2.46 μM and inhibited the growth of SW1116 cells with IC_{50} of 4.22 μM. While compound **11f** demonstrated potent inhibitory activity that inhibited the growth of HELA cells with IC_{50} of 7.30 μM and inhibited the growth of SW1116 cells with IC_{50} of 4.12 μM. Compound **8h** demonstrated the most potent inhibitory activity that inhibited the growth of HEPG2 cells with IC_{50} of 0.78 μM and inhibited the growth of SW1116 cells with IC_{50} of 1.47 μM, it also inhibited the activity of telomerase with IC_{50} of 1.24 μM, which was comparable to the positive control staurosporine.

In order to gain deeper understanding of the structure–activity relationships observed at the telomerase, molecular docking of the potent inhibitors **5c**, **8h** and **11f** into the binding site of telomerase was performed on the binding model based on the telomerase complex structure. Analysis of the three compounds binding conformation demonstrated that these compounds were stabilized by hydrogen bonding interaction with Arg194. Apoptosis assay showed the compounds were potential antitumor agents. The result provided valuable information for the design of telomerase inhibitors as antitumor agents.

4. Experimental section

4.1. Methods of synthesis

All the NMR spectra were recorded on a Bruker DPX 500 model Spectrometer in $CDCl_3$. Chemical shifts (δ) for ^1H NMR spectra were reported in parts per million to residual solvent protons. Melting points were measured on a Boetius micro melting point apparatus. The ESI-MS spectra were recorded on a Mariner System 5304 Mass spectrometer. All chemicals and reagents used in current study were of analytical grade. TLC was run on the silica gel coated aluminum sheets (Silica Gel 60 GF254, E. Merk, Germany) and visualized in UV light (254 nm).

4.1.1. General procedure for synthesis of the target compounds (5a–5k), (8a–8k) and (11a–11k)

To a solution of compound **4** (1 mmol) in acetone, the corresponding benzyl bromide compounds (1 mmol) were added and the mixture was stirred under reflux for 1–2 h in the presence of K_2CO_3 (1 mmol). Then, the solvent was removed under reduced pressure and a solid obtained. The solid was recrystallized from ethylalcohol to afford compounds **5a**–**5k**.

To a solution of compound **7** (1 mmol) in acetone, the corresponding benzyl bromide compounds (1 mmol) were added and the mixture was stirred under reflux for 1–2 h in the presence of K_2CO_3 (1 mmol). Then, the solvent was removed under reduced pressure and a solid obtained. The solid was recrystallized from ethylalcohol to afford compounds **8a**–**8k**.

To a solution of compound **10** (1 mmol) in acetonitrile, the corresponding benzyl bromide compounds (1 mmol) were added and the mixture was stirred under reflux for 4–8 h in the presence of NaOH (2 mmol). Then, the solvent was removed under reduced pressure and a solid obtained. The solid was recrystallized from acetonitrile to afford compounds **11a**–**11k**.

4.1.1.1. 2-((2-Fluorobenzyl)thio)-5-(pyrazin-2-yl)-1,3,4-oxadiazole (5a). White solid, yield 89%; mp: 142–143 °C. ^1H NMR (500 MHz, $CDCl_3$): 4.61 (s, 2H); 7.05–7.13 (m, 2H); 7.26–7.32 (m, 1H); 7.56 (t, J = 7.65 Hz, 1H); 8.73 (s, 2H); 9.42 (s, 1H). ESI-MS: 289.1 ($C_{13}H_{10}FN_4OS$, $[M+H]^+$). Anal. Calcd for $C_{13}H_9FN_4OS$: C, 54.16; H, 3.15; N, 19.43. Found: C, 54.31; H, 3.16; N, 19.49.

4.1.1.2. 2-((2-Chlorobenzyl)thio)-5-(pyrazin-2-yl)-1,3,4-oxadiazole (5b). White solid, yield 93%; mp: 75–76 °C. ^1H NMR (500 MHz, $CDCl_3$): 4.69 (s, 2H); 7.22–7.28 (m, 2H); 7.42 (d, J = 7.45 Hz, 1H); 7.65 (d, J = 7.20 Hz, 1H); 8.73 (s, 2H); 9.41 (s, 1H). ESI-MS: 305.0 ($C_{13}H_{10}ClN_4OS$, $[M+H]^+$). Anal. Calcd for $C_{13}H_9ClN_4OS$: C, 51.23; H, 2.98; N, 18.38. Found: C, 51.38; H, 2.97; N, 18.44.

4.1.1.3. 2-((2-Bromobenzyl)oxy)-5-(pyrazin-2-yl)-1,3,4-oxadiazole (5c). White solid, yield 91%; mp: 86–88 °C. ^1H NMR (500 MHz, $CDCl_3$): 4.71 (s, 2H); 7.16–7.22 (m, 1H); 7.30 (t, J = 7.50 Hz, 1H); 7.61 (d, J = 7.86 Hz, 1H); 7.68 (dd, J_1 = 1.65 Hz, J_2 = 6.03 Hz, 1H); 8.74 (s, 2H); 9.42 (s, 1H). ESI-MS: 349.0 ($C_{13}H_{10}BrN_4OS$, $[M+H]^+$). Anal. Calcd for $C_{13}H_9BrN_4OS$: C, 44.71; H, 2.60; N, 16.04. Found: C, 44.84; H, 2.59; N, 16.09.

4.1.1.4. 2-((3-Chlorobenzyl)thio)-5-(pyrazin-2-yl)-1,3,4-oxadiazole (5d). White solid, yield 88%; mp: 76–77 °C. ^1H NMR (500 MHz, $CDCl_3$): 4.53 (s, 2H); 7.26–7.29 (m, 2H); 7.37 (s, 1H); 7.48 (s, 1H); 8.73 (s, 2H); 9.42 (s, 1H). ESI-MS: 305.0 ($C_{13}H_{10}ClN_4OS$, $[M+H]^+$). Anal. Calcd for $C_{13}H_9ClN_4OS$: C, 51.23; H, 2.98; N, 18.38. Found: C, 51.11; H, 2.99; N, 18.45.

4.1.1.5. 2-((3-Bromobenzyl)thio)-5-(pyrazin-2-yl)-1,3,4-oxadiazole (5e). White solid, yield 92%; mp: 90–91 °C. ^1H NMR (500 MHz, $CDCl_3$): 4.54 (s, 2H); 7.20–7.27 (m, 1H); 7.30 (t, J = 7.68 Hz, 2H); 7.65 (s, 1H); 8.72–8.75 (m, 2H); 9.43 (s, 1H). ESI-MS: 349.0 ($C_{13}H_{10}BrN_4OS$, $[M+H]^+$). Anal. Calcd for $C_{13}H_9BrN_4OS$: C, 44.71; H, 2.60; N, 16.04. Found: C, 44.87; H, 2.59; N, 16.11.

4.1.1.6. 2-((4-Fluorobenzyl)thio)-5-(pyrazin-2-yl)-1,3,4-oxadiazole (5f). White solid, yield 90%; mp: 121–123 °C. ^1H NMR (500 MHz, $CDCl_3$): 4.55 (s, 2H); 7.15 (d, J = 7.90 Hz, 2H); 7.35 (d, J = 7.80 Hz, 2H); 8.72 (s, 2H); 9.42 (s, 1H). ESI-MS: 289.1 ($C_{13}H_{10}FN_4OS$, $[M+H]^+$). Anal. Calcd for $C_{13}H_9FN_4OS$: C, 54.16; H, 3.15; N, 19.43. Found: C, 54.32; H, 3.16; N, 19.48.

4.1.1.7. 2-((4-Chlorobenzyl)thio)-5-(pyrazin-2-yl)-1,3,4-oxadiazole (5g). White solid, yield 83%; mp: 118–119 °C. ^1H NMR (500 MHz, $CDCl_3$): 4.53 (s, 2H); 7.31 (d, J = 8.61 Hz, 2H); 7.42 (d, J = 8.40 Hz, 2H); 8.73 (s, 2H); 9.42 (s, 1H). ESI-MS: 305.0 ($C_{13}H_{10}ClN_4OS$, $[M+H]^+$). Anal. Calcd for $C_{13}H_9ClN_4OS$: C, 51.23; H, 2.98; N, 18.38. Found: C, 51.08; H, 2.99; N, 18.44.

4.1.1.8. 2-((2-Bromobenzyl)oxy)-5-(pyrazin-2-yl)-1,3,4-oxadiazole (5h). White solid, yield 91%; mp: 117–118 °C. ^1H NMR (500 MHz, $CDCl_3$): 4.51 (s, 2H); 7.36 (d, J = 8.25 Hz, 2H); 7.47 (d, J = 8.35 Hz, 2H); 8.73 (d, J = 6.70 Hz, 2H); 9.42 (s, 1H). ESI-MS: 349.0 ($C_{13}H_{10}BrN_4OS$, $[M+H]^+$). Anal. Calcd for $C_{13}H_9BrN_4OS$: C, 44.71; H, 2.60; N, 16.04. Found: C, 44.85; H, 2.61; N, 16.10.

4.1.1.9. 2-((2,4-Difluorobenzyl)thio)-5-(pyrazin-2-yl)-1,3,4-oxadiazole (5i). White solid, yield 85%; mp: 85–87 °C. ^1H NMR (500 MHz, $CDCl_3$): 4.58 (s, 2H); 6.83–6.92 (m, 2H); 7.55–7.62 (m, 1H); 8.75 (s, 2H); 9.43 (s, 1H). ESI-MS: 307.0 ($C_{13}H_9F_2N_4OS$, $[M+H]^+$). Anal. Calcd for $C_{13}H_8F_2N_4OS$: C, 50.98; H, 2.63; N, 18.29. Found: C, 51.11; H, 2.64; N, 18.33.

4.1.1.10. 2-((2,6-Difluorobenzyl)thio)-5-(pyrazin-2-yl)-1,3,4-oxadiazole (5j). White solid, yield 87%; mp: 72–73 °C. ^1H NMR (500 MHz, $CDCl_3$): 4.67 (s, 2H); 6.92–6.97 (m, 2H); 7.27–7.34 (m, 1H); 8.75 (s, 2H); 9.45 (s, 1H). ESI-MS: 307.0

($C_{13}H_9F_2N_4OS$, $[M+H]^+$). Anal. Calcd for $C_{13}H_8F_2N_4OS$: C, 50.98; H, 2.63; N, 18.29. Found: C, 51.08; H, 2.64; N, 18.23.

4.1.1.11. 2-(Benzylthio)-5-(pyrazin-2-yl)-1,3,4-oxadiazole (5k). White solid, yield 88%; mp: 79–80 °C. ^{1}H NMR (500 MHz, $CDCl_3$): 4.58 (s, 2H); 7.31–7.36 (m, 3H); 7.47 (d, J = 7.15 Hz, 1H); 8.72 (s, 2H); 9.42 (s, 1H). ESI-MS: 271.0 ($C_{13}H_{11}N_4OS$, $[M+H]^+$). Anal. Calcd for $C_{13}H_{10}N_4OS$: C, 57.76; H, 3.73; N, 20.73. Found: C, 57.61; H, 3.72; N, 20.78.

4.1.1.12. 2-((2-Fluorobenzyl)thio)-5-(pyrazin-2-yl)-1,3,4-thiadiazole (8a). White solid, yield 71%; mp: 120–121 °C. ^{1}H NMR (500 MHz, $CDCl_3$): 4.69 (s, 2H); 7.07–7.13 (m, 2H); 7.24–7.32 (m, 1H); 7.56 (t, J = 7.60 Hz, 1H); 8.59 (s, 1H); 8.66 (s, 1H); 9.54 (s, 1H). ESI-MS: 305.0 ($C_{13}H_{10}FN_4S_2$, $[M+H]^+$). Anal. Calcd for $C_{13}H_9FN_4S_2$: C, 53.10; H, 2.98; N, 18.41. Found: C, 53.28; H, 2.99; N, 18.47.

4.1.1.13. 2-((2-Chlorobenzyl)thio)-5-(pyrazin-2-yl)-1,3,4-thiadiazole (8b). White solid, yield 68%; mp: 116–117 °C. ^{1}H NMR (500 MHz, $CDCl_3$): 4.79 (s, 2H); 7.24–7.27 (m, 2H); 7.43 (d, J = 9.33 Hz, 1H); 7.63–7.66 (m, 1H); 8.63 (d, J = 17.76 Hz, 2H); 9.55 (s, 1H). ESI-MS: 321.0 ($C_{13}H_{10}ClN_4S_2$, $[M+H]^+$). Anal. Calcd for $C_{13}H_9ClN_4S_2$: C, 48.67; H, 2.83; N, 17.46. Found: C, 48.78; H, 2.82; N, 17.41.

4.1.1.14. 2-((2-Bromobenzyl)thio)-5-(pyrazin-2-yl)-1,3,4-thiadiazole (8c). White solid, yield 63%; mp: 133–135 °C. ^{1}H NMR (500 MHz, $CDCl_3$): 4.80 (s, 2H); 7.15–7.21 (m, 1H); 7.27–7.32 (m, 1H); 7.60–7.68 (m, 2H); 8.61 (s, 1H); 8.66 (s, 1H); 9.55 (s, 1H). ESI-MS: 365.0 ($C_{13}H_{10}BrN_4S_2$, $[M+H]^+$). Anal. Calcd for $C_{13}H_9BrN_4S_2$: C, 42.75; H, 2.48; N, 15.34. Found: C, 42.88; H, 2.49; N, 15.38.

4.1.1.15. 2-((3-Chlorobenzyl)thio)-5-(pyrazin-2-yl)-1,3,4-thiadiazole (8d). Yellow solid, yield 77%; mp: 127–128 °C. ^{1}H NMR (500 MHz, $CDCl_3$): 4.62 (s, 2H); 7.27–7.36 (m, 2H); 7.38–7.40 (m, 1H); 7.48 (s, 1H); 8.59–8.61 (m, 1H); 8.66 (s, 1H); 9.54 (s, 1H). ESI-MS: 321.0 ($C_{13}H_{10}ClN_4S_2$, $[M+H]^+$). Anal. Calcd for $C_{13}H_9ClN_4S_2$: C, 48.67; H, 2.83; N, 17.46. Found: C, 48.54; H, 2.84; N, 17.51.

4.1.1.16. 2-((3-Bromobenzyl)thio)-5-(pyrazin-2-yl)-1,3,4-thiadiazole (8e). White solid, yield 70%; mp: 120–121 °C. ^{1}H NMR (500 MHz, $CDCl_3$): 4.61 (s, 2H); 7.20–7.27 (m, 1H); 7.42 (s, 2H); 7.64 (s, 1H); 8.60 (s, 1H); 8.66 (s, 1H); 9.54 (s, 1H). ESI-MS: 365.0 ($C_{13}H_{10}BrN_4S_2$, $[M+H]^+$). Anal. Calcd for $C_{13}H_9BrN_4S_2$: C, 42.75; H, 2.48; N, 15.34. Found: C, 42.60; H, 2.49; N, 15.39.

4.1.1.17. 2-((4-Fluorobenzyl)thio)-5-(pyrazin-2-yl)-1,3,4-thiadiazole (8f). White solid, yield 72%; mp: 136–137 °C. ^{1}H NMR (500 MHz, $CDCl_3$): 4.61 (s, 2H); 7.12–7.17 (m, 2H); 7.36 (d, J = 7.80 Hz, 2H); 8.58 (s, 1H); 8.65 (s, 1H); 9.54 (s, 1H). ESI-MS: 305.0 ($C_{13}H_{10}FN_4S_2$, $[M+H]^+$). Anal. Calcd for $C_{13}H_9FN_4S_2$: C, 53.10; H, 2.98; N, 18.41. Found: C, 53.26; H, 2.99; N, 18.35.

4.1.1.18. 2-((4-Chlorobenzyl)thio)-5-(pyrazin-2-yl)-1,3,4-thiadiazole (8g). Yellow solid, yield 61%; mp: 153–155 °C. ^{1}H NMR (500 MHz, $CDCl_3$): 4.60 (s, 2H); 7.31 (d, J = 8.10 Hz, 2H); 7.41 (d, J = 7.90 Hz, 2H); 8.58 (s, 1H); 8.65 (s, 1H); 9.52 (s, 1H). ESI-MS: 321.0 ($C_{13}H_{10}ClN_4S_2$, $[M+H]^+$). Anal. Calcd for $C_{13}H_9ClN_4S_2$: C, 48.67; H, 2.83; N, 17.46. Found: C, 48.79; H, 2.84; N, 17.41.

4.1.1.19. 2-((4-Bromobenzyl)thio)-5-(pyrazin-2-yl)-1,3,4-thiadiazole (8h). Yellow solid, yield 68%; mp: 158–160 °C. ^{1}H NMR (500 MHz, $CDCl_3$): 4.59 (s, 2H); 7.37 (d, J = 8.61 Hz, 2H); 7.48 (d, J = 8.58 Hz, 2H); 8.59–8.61 (m, 1H); 8.66 (s, 1H); 9.54 (s, 1H). ESI-MS: 365.0 ($C_{13}H_{10}BrN_4S_2$, $[M+H]^+$). Anal. Calcd for $C_{13}H_9BrN_4S_2$: C, 42.75; H, 2.48; N, 15.34. Found: C, 42.88; H, 2.47; N, 15.38.

4.1.1.20. 2-((2,4-Difluorobenzyl)thio)-5-(pyrazin-2-yl)-1,3,4-thiadiazole (8i). White solid, yield 72%; mp: 140–142 °C. ^{1}H NMR (500 MHz, $CDCl_3$): 4.69 (s, 2H); 6.83–6.87 (m, 2H); 7.54–7.59 (m, 1H); 8.60 (s, 1H); 8.66 (s, 1H); 9.54 (s, 1H). ESI-MS: 323.0 ($C_{13}H_9F_2N_4S_2$, $[M+H]^+$). Anal. Calcd for $C_{13}H_8F_2N_4S_2$: C, 48.44; H, 2.50; N, 17.38. Found: C, 48.56; H, 2.51; N, 17.33.

4.1.1.21. 2-((2,6-Difluorobenzyl)thio)-5-(pyrazin-2-yl)-1,3,4-thiadiazole (8j). White solid, yield 68%; mp: 165–166 °C. ^{1}H NMR (500 MHz, $CDCl_3$): 4.74 (s, 2H); 6.92–6.95 (m, 2H); 7.28–7.33 (m, 1H); 8.60 (s, 1H); 8.67 (s, 1H); 9.56 (s, 1H). ESI-MS: 323.0 ($C_{13}H_9F_2N_4S_2$, $[M+H]^+$). Anal. Calcd for $C_{13}H_8F_2N_4S_2$: C, 48.44; H, 2.50; N, 17.38. Found: C, 48.60; H, 2.51; N, 17.34.

4.1.1.22. 2-(Benzylthio)-5-(pyrazin-2-yl)-1,3,4-thiadiazole (8k). White solid, yield 66%; mp: 127–128 °C. ^{1}H NMR (500 MHz, $CDCl_3$): 4.64 (s, 2H); 7.28–7.36 (m, 3H); 7.46 (d, J = 7.45 Hz, 2H); 8.58 (s, 1H); 8.64 (s, 1H); 9.53 (s, 1H). ESI-MS: 287.0 ($C_{13}H_{11}N_4S_2$, $[M+H]^+$). Anal. Calcd for $C_{13}H_{10}N_4S_2$: C, 54.52; H, 3.52; N, 19.56. Found: C, 54.61; H, 3.51; N, 19.62.

4.1.1.23. 2-(5-((2-Fluorobenzyl)thio)-4-phenyl-4H-1,2,4-triazol-3-yl)pyrazine (11a). Yellow solid, yield 74%; mp: 131–132 °C. ^{1}H NMR (500 MHz, $CDCl_3$): 4.64 (s, 2H); 7.01–7.10 (m, 2H); 7.16 (d, J = 7.35 Hz, 2H); 7.24–7.30 (m, 1H); 7.43–7.50 (m, 3H); 7.54 (t, J = 7.60 Hz, 1H); 8.24 (s, 1H); 8.49 (s, 1H); 9.39 (s, 1H). ESI-MS: 364.1 ($C_{19}H_{15}FN_5S$, $[M+H]^+$). Anal. Calcd for $C_{19}H_{14}FN_5S$: C, 62.79; H, 3.88; N, 19.27. Found: C, 62.61; H, 3.89; N, 19.33.

4.1.1.24. 2-(5-((2-Chlorobenzyl)thio)-4-phenyl-4H-1,2,4-triazol-3-yl)pyrazine (11b). Yellow solid, yield 77%; mp: 144–145 °C. ^{1}H NMR (500 MHz, $CDCl_3$): 4.69 (s, 2H); 7.13–7.16 (m, 2H); 7.19–7.26 (m, 2H); 7.35–7.38 (m, 1H); 7.41–7.49 (m, 3H); 7.61–7.64 (m, 1H); 8.24 (s, 1H); 8.49 (s, 1H); 9.38 (s, 1H). ESI-MS: 380.1 ($C_{19}H_{15}ClN_5S$, $[M+H]^+$). Anal. Calcd for $C_{19}H_{14}ClN_5S$: C, 60.07; H, 3.71; N, 18.44. Found: C, 60.21; H, 3.70; N, 18.40.

4.1.1.25. 2-(5-((2-Bromobenzyl)thio)-4-phenyl-4H-1,2,4-triazol-3-yl)pyrazine (11c). Yellow solid, yield 65%; mp: 160–162 °C. ^{1}H NMR (500 MHz, $CDCl_3$): 4.70 (s, 2H); 7.12–7.17 (m, 3H); 7.24–7.28 (m, 1H); 7.42–7.51 (m, 3H); 7.55 (d, J = 7.50 Hz, 1H); 7.64 (d, J = 7.50 Hz, 1H); 8.24 (s, 1H); 8.49 (s, 1H); 9.38 (s, 1H). ESI-MS: 424.0 ($C_{19}H_{15}BrN_5S$, $[M+H]^+$). Anal. Calcd for $C_{19}H_{14}BrN_5S$: C, 53.78; H, 3.33; N, 16.50. Found: C, 53.60; H, 3.34; N, 16.44.

4.1.1.26. 2-(5-((3-Chlorobenzyl)thio)-4-phenyl-4H-1,2,4-triazol-3-yl)pyrazine (11d). White solid, yield 78%; mp: 117–118 °C. ^{1}H NMR (500 MHz, $CDCl_3$): 4.55 (s, 2H); 7.15–7.17 (m, 2H); 7.23–7.27 (m, 2H); 7.38 (s, 1H); 7.45–7.51 (m, 4H); 8.25 (s, 1H); 8.50 (s, 1H); 9.39 (s, 1H). ESI-MS: 380.1 ($C_{19}H_{15}ClN_5S$, $[M+H]^+$). Anal. Calcd for $C_{19}H_{14}ClN_5S$: C, 60.07; H, 3.71; N, 18.44. Found: C, 59.92; H, 3.70; N, 18.49.

4.1.1.27. 2-(5-((3-Bromobenzyl)thio)-4-phenyl-4H-1,2,4-triazol-3-yl)pyrazine (11e). Yellow solid, yield 67%; mp: 135–136 °C. ^{1}H NMR (500 MHz, $CDCl_3$): 4.50 (s, 2H); 7.14–7.18 (m, 3H); 7.34 (d, J = 7.60 Hz, 1H); 7.39 (d, J = 7.90 Hz, 1H); 7.44–7.51 (m, 3H); 7.52 (s, 1H); 8.24 (s, 1H); 8.49 (s, 1H); 9.38 (s, 1H). ESI-MS: 424.0 ($C_{19}H_{15}BrN_5S$, $[M+H]^+$). Anal. Calcd for $C_{19}H_{14}BrN_5S$: C, 53.78; H, 3.33; N, 16.50. Found: C, 53.89; H, 3.34; N, 16.45.

4.1.1.28. 2-(5-((4-Fluorobenzyl)thio)-4-phenyl-4H-1,2,4-triazol-3-yl)pyrazine (11f). White solid, yield 76%; mp: 144–145 °C.

^{1}H NMR (500 MHz, $CDCl_3$): 4.59 (s, 2H); 7.10–7.16 (m, 4H); 7.28 (s, 2H); 7.37–7.49 (m, 3H); 8.24 (s, 1H); 8.49 (s, 1H); 9.38 (s, 1H). ESI-MS: 364.1 ($C_{19}H_{15}FN_5S$, $[M+H]^+$). Anal. Calcd for $C_{19}H_{14}FN_5S$: C, 62.79; H, 3.88; N, 19.27. Found: C, 62.62; H, 3.89; N, 19.34.

4.1.1.29. 2-(5-((4-Chlorobenzyl)thio)-4-phenyl-4H-1,2,4-triazol-3-yl)pyrazine (11g). Yellow solid, yield 77%; mp: 169–170 °C. ^{1}H NMR (500 MHz, $CDCl_3$): 4.52 (s, 2H); 7.14 (d, J = 6.78 Hz, 1H); 7.24 (s, 1H); 7.27 (s, 1H); 7.34 (d, J = 8.43 Hz, 2H); 7.44–7.48 (m, 4H); 8.23 (s, 1H); 8.49 (s, 1H); 9.37 (s, 1H). ESI-MS: 380.1 ($C_{19}H_{15}ClN_5S$, $[M+H]^+$). Anal. Calcd for $C_{19}H_{14}ClN_5S$: C, 60.07; H, 3.71; N, 18.44. Found: C, 60.18; H, 3.70; N, 18.39.

4.1.1.30. 2-(5-((4-Bromobenzyl)thio)-4-phenyl-4H-1,2,4-triazol-3-yl)pyrazine (11h). White solid, yield 72%; mp: 167–169 °C. ^{1}H NMR (500 MHz, $CDCl_3$): 4.52 (s, 2H); 7.16 (d, J = 6.75 Hz, 2H); 7.34 (d, J = 10.05 Hz, 2H); 7.41–7.53 (m, 5H); 8.24 (s, 1H); 8.50 (s, 1H); 9.39 (s, 1H). ESI-MS: 424.0 ($C_{19}H_{15}BrN_5S$, $[M+H]^+$). Anal. Calcd for $C_{19}H_{14}BrN_5S$: C, 53.82; H, 3.33; N, 16.51. Found: C, 53.69; H, 3.32; N, 16.46.

4.1.1.31. 2-(5-((2,4-Difluorobenzyl)thio)-4-phenyl-4H-1,2,4-triazol-3-yl)pyrazine (11i). Yellow solid, yield 80%; mp: 156–157 °C. ^{1}H NMR (500 MHz, $CDCl_3$): 4.56 (s, 2H); 6.77–6.84 (m, 2H); 7.17–7.21 (m, 2H); 7.44–7.51 (m, 3H); 7.57 (dd, J_1 = 8.40 Hz, J_2 = 14.95 Hz, 1H); 8.24 (s, 1H); 8.49 (s, 1H); 9.39 (s, 1H). ESI-MS: 382.1 ($C_{19}H_{14}F_2N_5S$, $[M+H]^+$). Anal. Calcd for $C_{19}H_{13}F_2N_5S$: C, 59.83; H, 3.44; N, 18.36. Found: C, 59.67; H, 3.45; N, 18.42.

4.1.1.32. 2-(5-((2,6-Difluorobenzyl)thio)-4-phenyl-4H-1,2,4-triazol-3-yl)pyrazine (11j). Yellow solid, yield 78%; mp: 172–173 °C. ^{1}H NMR (500 MHz, $CDCl_3$): 4.59 (s, 2H); 6.87 (t, J = 7.80 Hz, 2H); 7.21–7.24 (m, 3H); 7.44–7.48 (m, 3H); 8.24 (s, 1H); 8.49 (s, 1H); 9.40 (s, 1H). ESI-MS: 382.1 ($C_{19}H_{14}F_2N_5S$, $[M+H]^+$). Anal. Calcd for $C_{19}H_{13}F_2N_5S$: C, 59.83; H, 3.44; N, 18.36. Found: C, 59.97; H, 3.45; N, 18.30.

4.1.1.33. 2-(5-(Benzylthio)-4-phenyl-4H-1,2,4-triazol-3-yl)pyrazine (11k). Yellow solid, yield 86%; mp: 140–141 °C. ^{1}H NMR (500 MHz, $CDCl_3$): 4.58 (s, 2H); 7.13 (d, J = 7.65 Hz, 2H); 7.26–7.29 (m, 3H); 7.38 (d, J = 7.50 Hz, 1H); 7.42–7.48 (m, 3H); 8.24 (s, 1H); 8.49 (s, 1H); 9.38 (s, 1H). ESI-MS: 346.1 ($C_{19}H_{16}N_5S$, $[M+H]^+$). Anal. Calcd for $C_{19}H_{15}N_5S$: C, 66.07; H, 4.38; N, 20.27. Found: C, 66.21; H, 4.39; N, 20.32.

4.2. Cell proliferation assay

The antitumor activities of compounds **5a**–**5k**, **8a**–**8k** and **11a**–**11k** were determined using a standard (MTT)-based colorimetric assay (Sigma). Seed 10^4 cells per well into 96-well plates, incubate at 37 °C, 5% CO_2 for 24 h. Then add 100 μL a series concentration of drug-containing medium into wells to maintain the final concentration of drug as 30, 10, 3.33, 1.11, 0.37 and 0.12 μg/mL. One concentration should be triplicated and staurosporine was used for the positive control. After 48 h, cell survival was determined by the addition of an MTT solution (25 μL of 5 mg/mL MTT in PBS). After 4 h, discard the medium and add 100 μL DMSO; the plates were votexed for 10 min to make completely dissolution. Optical absorbance was measured at 490 nm.

4.3. Telomerase inhibitory assay

Compounds were tested in a search for small molecule inhibitors of telomerase activity by using the TRAP–PCR–ELISA assay. In detail, the HEPG2 cells were firstly maintained in DMEM medium (GIBCO, New York, USA) supplemented with 10% fetal bovine serum (GIBCO, New York, USA), streptomycin (0.1 mg/mL) and penicillin (100 IU/mL) at 37 °C in a humidified atmosphere containing 5% CO_2. After trypsinization, 5×10^4 cultured cells in logarithmic growth were seeded into T25 flasks (Corning, New York, USA) and cultured to allow to adherence. The cells were then incubated with Staurosporine (Santa Cruz, Santa Cruz, USA) and the drugs with a series of concentration as 30, 10, 3.33, 1.11, 0.37 and 0.12 μg/mL, respectively. After 24 h treatment, the cells were harvested by cell scraper orderly following by washed once with PBS. The cells were lysed in 150 μL RIPA cell lysis buffer (Santa Cruz, Santa Cruz, USA), and incubated on ice for 30 min. The cellular supernatants were obtained via centrifugation at 12,000 g for 20 min at 4 °C and stored at −80 °C.

The TRAP–PCR–ELISA assay was performed using a telomerase detection kit (Roche, Basel, Switzerland) according to the manufacturer's protocol. In brief, 2 μL of cell extracts were mixed with 48 μL TRAP reaction mixtures. PCR was then initiated at 94 °C, 120 s for pre-denaturation and performed using 35 cycles each consisting of 94 °C for 30 s, 50 °C for 30 s, 72 °C for 90 s. Then 20 μL of PCR products were hybridized to a digoxigenin (DIG)-labeled telomeric repeat specific detection probe. And the PCR products were immobilized via the biotin-labeled primer to a streptavidin-coated microtiter plate subsequently. The immobilized DNA fragment were detected with a peroxidase-conjugated anti-DIG antibody and visualized following addition of the stop regent. The microtitre plate was assessed on TECAN Infinite M200 microplate reader (Männedorf, Switzerland) at a wavelength of 490 nm, and the final values were presented.

4.4. Apoptosis assay

HEPG2 cells were treated with various concentrations of compound **8h** for 24 h and then stained with both Annexin V-FITC (fluorescein isothiocyanate) and propidium iodide (PI). Then samples were analyzed by FACSCalibur flow cytometer (Becton Dickinson, SanJose, CA).

4.5. Molecular docking study

Molecular docking of compounds into the 3D telomerase complex structure (PDB code:3DU6) was carried out using the Discovery Studio (version 3.1) as implemented through the graphical user interface DS-CDocker protocal.

The three-dimensional structures of the aforementioned compounds were constructed using Chem 3D ultra 12.0 software [Chemical Structure Drawing Standard; Cambridge Soft corporation, USA (2010)], then they were energetically minimized by using MMFF94 with 5000 iterations and minimum RMS gradient of 0.10. The crystal structures of telomerase complex were retrieved from the RCSB Protein Data Bank (http://www.rcsb.org/pdb/home/home.do). All bound water and ligands were eliminated from the protein and the polar hydrogen was added. Types of interactions of the docked protein with ligand were analyzed after the end of molecular docking.

4.6. Crystal structure determination

Crystal structure determination of compounds **5k**, **8k**, **11e** and **11i** were carried out on a Nonius CAD4 diffractometer equipped with graphitemonochromated Mo Kα (λ = 0.71073 Å) radiation (Table 1). The structure was solved by direct methods and refined on F^2 by fullmatrix least-squares methods using SHELX-97.[31] All non-hydrogen atoms of compounds **5k**, **8k**, **11e** and **11i** were refined with anisotropic thermal parameters. All hydrogen atoms were placed in geometrically idealized positions and constrained to ride on their parent atoms.

Acknowledgments

The work was financed by National Natural Science Foundation of China (No. J1103512).

References and notes

1. Deville, L.; Hillion, J.; Segal-Bendirdjian, E. *Biochim. Biophys. Acta* **2009**, *1792*, 229.
2. Huang, H. S.; Chiou, J. F.; Fong, Y.; Hou, C. C.; Lu, Y. C.; Wang, J. Y.; Shih, J. W.; Pan, Y. R.; Lin, J. J. *J. Med. Chem.* **2003**, *46*, 3300.
3. Philippi, C.; Loretz, B.; Schaefer, U. F.; Lehr, C. M. *J. Control. Release* **2010**, *146*, 228.
4. Lee, C. C.; Huang, K. F.; Lin, P. Y.; Huang, F. C.; Chen, C. L. *J. Med. Chem.* **2012**, *47*, 323.
5. Gillis, A. J.; Schuller, A. P.; Skordalakes, E. *Nature* **2008**, *455*, 633.
6. Singh, A. K.; Kumar, P.; Yadav, M.; Pandey, D. S. *J. Organomet. Chem.* **2010**, *695*, 567.
7. Zhao, X. H.; Liu, S. S.; Li, Y. Z.; Chen, M. D. *Spectrochim. Acta* **2010**, *75*, 794.
8. Asaki, T.; Hamamoto, T.; Sugiyama, Y.; Kuwano, K.; Kuwabara, K. *Bioorg. Med. Chem.* **2007**, *15*, 6692.
9. Corbett, J. W.; Rauckhorst, M. R.; Qian, F.; Hoffman, R. L.; Knauer, C. S.; Fitzgerald, L. W. *Bioorg. Med. Chem. Lett.* **2007**, *17*, 6250.
10. Tan, T. M. C.; Chen, Y.; Kong, K. H.; Bai, J.; Li, Y.; Lim, S. G.; Ang, T. H.; Lam, Y. *Antivir. Res.* **2006**, *71*, 7.
11. Gaonkar, S. L.; Rai, K. M. L.; Prabhuswamy, B. *Eur. J. Med. Chem.* **2006**, *41*, 841.
12. Li, Y.; Liu, J.; Zhang, H.; Yang, X.; Liu, Z. *Bioorg. Med. Chem. Lett.* **2006**, *16*, 2278.
13. Loetchutinat, C.; Chau, F.; Mankhetkorn, S. *Chem. Pharm. Bull.* **2003**, *51*, 728.
14. Kumar, D.; Sundaree, S.; Johnson, E. O.; Shah, K. *Bioorg. Med. Chem. Lett.* **2009**, *29*, 4492.
15. Khan, M. T.; Choudhary, M. I.; Khan, K. M.; Rani, M.; Rahman, A. U. *Bioorg. Med. Chem.* **2005**, *13*, 3385.
16. Guimaraes, C. R. W.; Boger, D. L.; Jorgensen, W. L. *J. Am. Chem. Soc.* **2005**, *127*, 17377.
17. Matysiak, J. *Eur. J. Med. Chem.* **2007**, *42*, 940.
18. Pan, Y.; Zhang, J. Z.; Li, X.; Chin, J. *J. Struct. Chem.* **2011**, *30*, 1001.
19. Du, H. T.; Du, H.; Chin, J. *J. Org. Chem.* **2010**, *30*, 137.
20. Schenone, S.; Brullo, C.; Bruno, O.; Bondavalli, F.; Ranise, A.; Filippelli, W.; Rinaldi, B.; Capuano, A.; Falcone, G. *Bioorg. Med. Chem.* **2006**, *14*, 1698.
21. Zhao, Y.; Ouyang, G. P.; Xu, W. M.; Jin, L. H.; Yuan, K. *Chin. J. Org. Chem.* **2010**, *30*, 2011.
22. Bhat, K. S.; Poojary, B.; Prasad, D. J.; Nalk, B.; Holla, B. S. *Eur. J. Med. Chem.* **2009**, *44*, 5066.
23. Sahoo, P. K.; Sharma, R.; Pattanayak, P. *Med. Chem. Res.* **2010**, *19*, 127.
24. Bayrak, H.; Demirbas, A. *Eur. J. Med. Chem.* **2009**, *44*, 1057.
25. Sztanke, K.; Tuzimski, T. *Eur. J. Med. Chem.* **2008**, *43*, 404.
26. Romagnoli, R.; Baraldi, P. G. *J. Med. Chem.* **2010**, *53*, 4248.
27. Zhang, Q.; Peng, Y. Y.; Wang, X. I. *J. Med. Chem.* **2007**, *50*, 749.
28. Ouyang, X.; Chen, X. *Bioorg. Med. Chem. Lett.* **2005**, *15*, 5154.
29. Zheng, Q. Z.; Zhang, X. M.; Xu, Y.; Chen, K.; Cai, Y. J.; Zhu, H. L. *Bioorg. Med. Chem.* **2010**, *18*, 7836.
30. Zhang, X. M.; Qiu, M.; Sun, J.; Zhang, Y. B.; Yang, Y. S.; Wang, X. L.; Tang, J. F.; Zhu, H. L. *Bioorg. Med. Chem.* **2011**, *19*, 6518.
31. Sheldrick, G. M. *SHELX-97, Program for X-ray Crystal Structure Solution and Refinement*; Göttingen University: Germany, 1997.